UV-induced formation of DNA damage in cells and their mutational consequences

Thierry Douki, S Adar

Chapter 7: UV-induced formation of DNA damage in cells and their mutational consequences.

T. Douki[a*], and S. Adar[b*]

[a] Univ. Grenoble Alpes, CEA, CNRS, IRIG, SyMMES, F-38000 Grenoble

[b] Department of Microbiology and Molecular Genetics, The Institute for Medical Research Israel–Canada, The Faculty of Medicine, The Hebrew University of Jerusalem, Ein Kerem, Jerusalem, 91120, Israel

*co-corresponding authors email address: thierry.douki@cea.fr & sheeraa@ekmd.huji.ac.il

ABSTRACT

Ultraviolet radiation induces a wide variety of damage in DNA that can originate from either photochemical reaction triggered by absorption of photons by DNA bases or oxidation processes mostly induced by photosensitization. The nature of DNA damage is dependent of numerous factors such the wavelength, the sequence, the chromatin structure or the cell type. The present chapter provides a summary of the available quantitative information of the yield of UV-induced DNA damage as well as the most recent pieces of information bases on state-of-the-art techniques such as next generation sequencing. The mutational consequences of the DNA photoproducts are briefly discussed.

Table of Contents

7.1 Introduction

Information gathered over the years in model systems and isolated DNA made possible the identification the most relevant types of DNA damage that could be generated in cells upon exposure to UV radiation. They are either dimeric photoproducts involving adjacent pyrimidine bases or oxidatively generated lesions such as strand breaks and oxidized bases (Fig. 7.1). In the early 1960's, radioactivity-based assays were developed to quantify thymine-containing cyclobutane pyrimidine dimers (CPDs). The subsequent development of immunoassays made possible the collection of large amounts of information in various cellular systems and in skin not only on CPDs but also on pyrimidine (6-4) photoproducts (64-PPs) and their Dewar valence isomers (Dewars) [1, 2]. More specific methods based on molecular biology approaches [3] or mass spectrometry detection [4] provided data on the individual formation of each dimer at the different bipyrimidine sites. In the recent years, the breakthrough made in next generation sequencing provided an unprecedented picture on the formation and repair of DNA in the different region of chromatin [5, 6]. Information on oxidatively generated lesions was mostly obtained through electrophoretic-based assay such as the comet assay [7] or alkaline elution [8]. These methods were primarily developed for the quantification of strand breaks but could be extended to damaged bases by the use of purified DNA *N*-glycosylases that recognize well-defined classes of damage. Some specific lesions like 8-oxo-7,8-dihydroguanine (8-oxoGua) were also quantified by chromatographic approaches. The purpose of this chapter is to combine all these pieces of information, with emphasis placed on the most recent results but without neglecting relevant earlier data, in order to provide insight into the distribution of the most frequent UV-induced damage. Factors such as the cell type, the spectrum of the incident light and the specificity of the formation of damage in skin are also discussed.

Last, a short overview of link between DNA damage and mutagenesis is provided, especially in the light of recent next generation sequencing data.

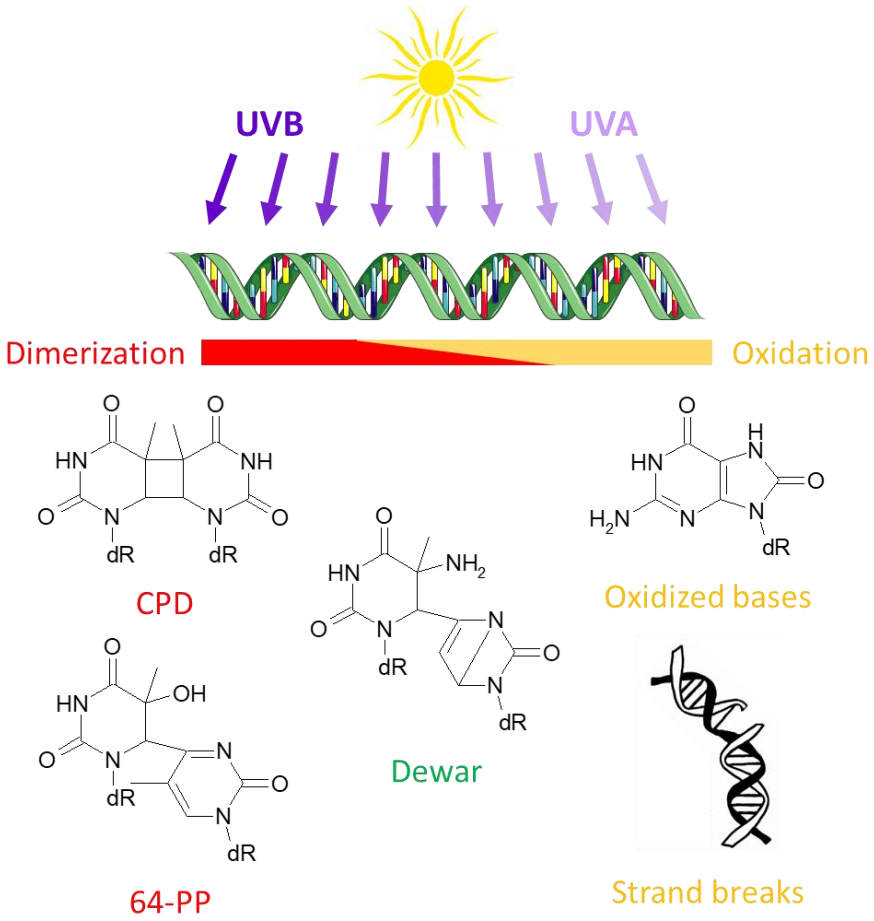

Figure 7.1: Chemical structure of the main DNA damage induced by UV radiation. UVB mostly leads to the formation of pyrimidine dimers while UVA is at the origin of a strong oxidative stress. However, as discussed in the present chapter, the boundary between the two wavelengths ranges is less tight that long believed.

7.2 UV-induced pyrimidine dimers in cellular DNA

UV radiation is an efficient DNA damaging agent but the yield and the nature of the photodamage strongly depend on the wavelength of the incident photons. Major attention has been paid to the UVA (320-400 nm) and UVB ranges (280-320 nm), which represent more than 95% and less than 5% of solar UV, respectively. Information is also available on the DNA damaging effects of UVC light (100-280 nm), which is closer to the UV absorption maximum of DNA at 260 nm.

7.2.1 Wavelength-dependent formation of pyrimidine dimers by UVB

7.2.1.1 CPDs and UVB radiation

The most efficient portion of the solar spectrum for the induction of pyrimidine dimers is UVB. This is easily explained by the fact that the wavelength of the most energetic photons in solar UV is closer to the maximal absorption of DNA (260 nm). Consequently, DNA base may absorb these photons and reach excited states, thereby opening the way to photochemical reaction as addressed by Martinez-Fernandeza and Improta in chapter 2 of this volume. Numerous data are available for CPDs. In cultured cells, the reported yields for broadband UVB lamps varies from 0.01 to 0.06 CPD/10^5 bases per J/m^2 [9-12]. The differences between these values can be explained by both the use of different analytical tools, the cell type and the emission spectrum of the UVB sources. The latter point is a major issue because the yield of the pyrimidine dimers varies along the UVB range. Action spectra in cultured human fibroblasts [13] show that the yield of CPD is in a 1 / 0.4 / 0.06 ratio at 280, 290 and 300 nm, respectively. In CHO cells, ratio of 1 / 0.22 / 0.01 were determined for the yield of CPD at 290, 300 and 310 nm [8]. These values show that the slightest increase in wavelength leads to a significant decrease in the yield of CPDs. They explain the difference in DNA damaging properties of sunlight depending on the hour the day, the latitude and the longitude. When the intensity on the UV radiation decreases as the result of the filter effect of the atmosphere, the ratio between the intensities of UVB and UVA is reduced [14, 15]. Differences in emission spectra is also of outmost importance when comparing results obtained by different teams using different irradiator.

7.2.1.2 Distribution of pyrimidine dimers in UVB irradiated cells

Most of the data discussed above are related to CPDs measured as a whole by immunoassays or to the sole TT CPD quantified by specific techniques. Yet, work on model systems and isolated DNA has shown that CPDs are formed at the four bipyrimidine sequences [4, 16]. These works also showed that, because of steric constraints, only the *cis,syn* diastereoisomer of CPD is detected in double-stranded DNA while other derivatives are produced in dinucleoside monophosphates and single-stranded DNA. Similar observations were made in cells with the following decreasing order of frequency for the *cis,syn* CPD: TT > TC > CT > CC [10, 17-25]. The ratio between the yields of these CPDs is 10 / 5 / 3 / 1, respectively. 64-PPs are also produced in significant amount by UVB radiation, although in a 3 to 5 lower yield than CPDs [9, 10, 12, 26]. In UVB-irradiated cultured cells, they are formed in detectable amounts only at TT and TC sites in a 1 to 5 ratio [9, 10, 21, 22, 24, 27]. CT and CC 64-PPs [21] have been detected in small amounts only upon UVC-irradiation of isolated DNA. The ratio between CPD and 64-PP is also dependent on the involved pyrimidine bases, with an approximate ratio of 10 at TT and 1 at TC sites. The ratio between all these different bipyrimidine photoproducts is constant from one mammalian cell type to the other. This reflects that the photochemistry of DNA is hardly modulated by the cellular environment. As detailed below, recent works based on the detection of pyrimidine dimers at the nucleotide resolution by next generation sequencing led to similar results [6, 28-31].

The only parameter that was found to drastically affect the mean distribution of CPDs in cells is the GC content of DNA [32]. This mostly concerns bacteria since all eukaryotic cells exhibit similar proportions of G/C and A/T bases pairs. Interestingly, this study of the impact of the GC content of DNA on the formation of pyrimidine dimers led to the conclusion that TC rather than TT dinucleotides are the most reactive sites in DNA. On a local scale, the reactivity of bipyrimidine sites can be modulated by the methylation

of cytosine, an important epigenetic event. Evidence are accumulating for an increased formation of damage at methylated CpG island [33], which is associated with increased mutagenesis [17, 23, 34, 35].

It may be mentioned than UVB may also trigger a secondary photoreaction within 64-PPs: the conversion into a Dewar valence isomer of the pyrimidone ring [36-39]. This has been well documented in model systems but is observed in very low yield in cells exposed to biologically relevant doses of UVB. As discussed later in this chapter, formation of Dewar in cells requires both UVB and UVA. Another important secondary reaction is the hydrolytic deamination of cytosine moieties in CPDs and CT and CC 64-PPs and Dewars [40-42]. This process leads to the formation of uracil-containing CPDs that play a role in mutagenesis, which is dominated by C→T mutations at bipyrimidic sites as discussed later in this chapter. More information on this process can be found in chapter 8 by Taylor and colleagues in this book.

7.2.2 UVA-induced CPDs

7.2.2.1 Direct formation of CPD upon exposure to UVA

Formation of CPDs is not only induced by UVB but also by the less energetic UVA. This photoreaction has long been neglected because UVA radiation was thought not to be absorbed by DNA. Yet, precise spectroscopic studies showed that DNA was actually a chromophore for UVA with an absorption at 350 nm respectively 10^4 and 10^3 times lower than at 280 and 300 nm [43]. Formation of CPDs in cellular DNA upon exposure to UVA has first been reported in bacteria [44]. Since then, similar results were obtained in cultured rodent cells [8, 12, 45, 46] as well as in human fibroblasts [47], keratinocytes [22, 48] and melanocytes [49]. The same observation was made in whole human skin both *in vivo* [50] and *ex vivo* [22, 24, 51]. The ratio between the yield of CPDs

after exposure to UVB or UVA is in the same range than the difference in absorption (Table 7.1). This value differs from one work to the other, which can be explained by differences in emission spectra of the UV sources. The importance of this parameter is clearly illustrated in action spectra where values of 60 were found between the ratio at 365 nm compared to either 290 nm or 310 nm in CHO cells [8]. Similarly, a ratio of 6 was determined for the yield of CPD in keratinocytes exposed at 302 nm compared to either 365 or 334 nm [47]. The correlation between the yield of CPDs and the DNA absorption, combined with the observation of CPD in UVA-irradiated isolated DNA, strongly suggests that a direct photochemical rather than a photosensitized process is involved in the UVA-induction of CPD [12, 52-54]. A last worth mentioning feature of the UVA photochemistry of DNA is that 64-PPs are at the best minor photoproducts. This can be explained by the change in the nature of the excited states generated when the wavelength of the absorbed photons increases from UVB to UVA [55].

Table 7.1: Comparison of the induction of CPDs in various cell types exposed to UVB and UVA radiations. The reported results are the ratio between the yields of formation.

Cell type	UV sources*	ratio	ref
CHO cells	290 vs 365 nm 310 vs 365 nm	40000 700	8
CHO cells	bb-UVB vs bb-UVA	700	12
CHO cells	bb-UVB vs bb-UVA	2000	46
Human skin fibroblasts	302 vs 334 nm 302 vs 365 nm	150 1000	47
Human keratinocytes	bb-UVB vs bb-UVA	20000	9
Human skin explants	bb-UVB vs bb-UVA	6500	22
Human skin explants phototype IV Human skin explants phototype II	bb-UVB vs bb-UVA	1100 1050	24

*bb: broadband

7.2.2.2 Dark CPDs

In addition to the formation of CPDs resulting from the weak but real absorption of UVA photons by DNA, UVA was reported to trigger a delayed formation of CPDs. This phenomenon was first reported in cultured melanocytes [56] and further extended to keratinocytes [57]. In both cell types, an oxidative pathway seems to be involved as shown by the inhibiting effects of antioxydants. Mechanistic studies have been performed in melanocytes. In this cell type UVA, and to a lesser extent UVB, were found to induce the formation of dark CPDs in the hours following irradiation of pigmented melanocytes but not of melanocytes originating from albino mice [56]. Interestingly, not only TT but also the mutagenic TC and CT CPDs were formed by this delayed mechanism. Evidence for a role of oxidation products of melanin and melanin precursor was provided by the replication of this effect on model systems involving oxidizing species, melanin derivatives and isolated DNA. A proposed mechanism is thus the formation of endoperoxide by UVA-induced oxidative stress that would then decompose into excited ketones. Such a mechanism has been previously described for oxidatively generated lesions [58]. It could induce the formation of CPDs by triplet energy transfer if the energy of the excited ketone is large enough. This pathway remains yet to be completely established in order to explain why C-containing dark CPDs are produced in significant amounts while photosensitized triplet-triplet energy transfer leads to the overwhelming formation of TT-CPD [59-61]. The biological relevance of this process was assessed by the observation of dark CPDs in human skin *in vivo* [62]. Their formation was observed even at the highest UVA wavelengths but not in the visible range [63]. An interesting phenomenon is the fast decrease in the peak of CPDs following exposure [56, 57, 62]. This could be explained by a faster repair of dark than immediate CPDs. Formation of dark CPDs requires molecular contact between

endoperoxides and bases. It is therefore favoured in open regions of chromatin where DNA repair is the most efficient. Further work is necessary to confirm this hypothesis that would help quantifying the biological role of dark CPDs.

7.2.3 UVC-induced DNA damage

7.2.3.1 Interest of UVC in photobiology

UVC is absent from the sunlight reaching the surface of Earth and of limited interest in terms of health effects. However, the recent COVID pandemic has led to a regain of interest in the UVC-mediated disinfection technologies [64]. This strategy has been used for many years, with a first germicidal action spectra published as early as 1946 [65] and confirmed since then by countless works. The maximal efficacy of UVC radiation is observed at 260-265 nm. In practical applications, equipment use the easily available 254 nm-emitting high-pressure mercury lamp. Its efficacy at this wavelength is approximately 90% of that at 260 nm. Because 254 nm radiation exhibits severe risks for skin and eyes [66], very recent alternatives have been proposed based on higher energy UVC, mostly at 222 nm. Because they exhibit a lower penetration in tissues, these photons are expected to be less damaging than 254 nm. It remains though to determine whether this represents an industrial advantage since all sterilization devices are protected. One novelty would be to use 222 nm light to directly sterilize areas of the human body but much deeper investigation on the harmlessness of these technologies would be necessary. More local application such as surgery site are yet interesting [67].

7.2.3.2 DNA damage in the UVC range

Exposure to 254 nm radiation exhibits its germicidal properties because it induces large amounts of damage in the genome of bacteria, yeasts and viruses. This is clearly

documented by early works on the formation of pyrimidine dimers in DNA [16, 68]. This was mostly motivated by the availability of mercury lamps emitting photons with a wavelength close to the maximal absorption of DNA. Today, UVC is mostly used in biological studies as a convenient tool for the fast production of significant amounts of DNA damage. Because it is more efficiently absorbed than UVB, UVC leads to a larger yield of photodamage. The ratio in UVC-induced yield with respect to UVB is around 10 in bacteria [11]. This trend is different in human skin because UVC is strongly absorbed by the stratum corneum and the upper layer of the cutaneous tissue. The yield of CPDs was found to be similar at 260 and 300 nm in the epidermis and almost 1 order of magnitude lower in the dermis [69]. Interestingly, the same decrease in the action spectrum in the UVC range compared to UVB is observed for skin cancer [70]. The proportion between the frequencies of the different photoproducts is the same in the UVC range than with UVB [21]. It should be stressed that this analogy holds only for low doses of UVC. Indeed, at this wavelength, secondary photoreactions can take place, in particular for CPDs. The 260 nm absorption of pyrimidine bases is lost upon formation of the cyclobutane dimer but the resulting CPDs keep an absorption band at approximately 230 nm with residual absorption at 254 nm. CPDs are thus able to absorb photons at this wavelength, which triggers a photoreversion reaction into the original bases [71, 72]. As a result, the dose-dependent formation is not linear but reaches a plateau [21, 73]. This phenomenon does not take place with UVB that is not absorbed by CPDs. Because photoreversion of 64-PPs does not occur, the ratio between CPDs and 64-PPs decreases as the UVC dose increases. An additional issue is that C-containing CPDs are more susceptible to photoreversion than TT CPD [21, 72]. Therefore, the ratio between the levels of the four possible CPDs also varies at large UVC dose. Although most data on UVC-induced photodamage in double stranded B-DNA were

obtained at 254 nm, data are available for lower wavelengths for isolated DNA. It was thus shown that the yields of CPD at 220 and 240 nm represent 80 and 40% of that at 260 nm, respectively [74]. In the 170-200 nm region, where DNA exhibits a second absorption maximum, the yield of CPD is slightly larger than that determined at 260 nm [74]. In skin, exposure to 222 nm did not lead to formation of CPDs, in contrast to UVB and, to a lesser extent, to 254 nm radiation [75]. Works carried out on isolated DNA provided information on the effect of higher energy UVC, typically 195 nm. At this wavelength, direct ionization of DNA bases is highly efficient and leads to damage of oxidative origin mostly observed at guanine bases. Their yields is a 6-fold larger yield than that of CPDs [76, 77].

7.2.3.3 Photochemistry in bacterial spores

Like bacteria, yeasts and other microorganisms, bacterial spores are killed upon UVC sterilization as the result of massive induction of DNA damage. A major difference is the nature of the induced photoproducts. In contrast to all other living cells, exposure of spores to UV radiation does not lead to the formation of CPDs and 64-PPs but to a dimer involving two adjacent thymine bases, 5-(α-thyminyl)-thymine also known as the spore photoproduct (SP) [78]. This specific photochemistry is explained by the unusual A-like form of DNA in spores [79-81]. This conformation is induced by the highly dehydrated core environment and the complexation of large amounts of small acid soluble proteins to DNA. In addition, the spore is loaded with large concentrations of dipicolinate that favour the formation of SP [82, 83]. Like CPDs, SP is produced in maximum yield at the maximal absorption of DNA [84]. However, it is produced at higher energy (222 nm) in significant yield [85]. Formation of SP is believed to explain the photoresistance of spores since a very efficient radical-SAM (*S*-adenosyl-methionine) repair enzyme is present in the spore and rapidly reverts SP upon germination [86].

7.3 Oxidatively generated DNA damage in cells

Emphasized has been placed in part 2 on the formation of pyrimidine dimers. Sunlight is also known to induce DNA damage through oxidative pathways. The underlying mechanisms have been documented by many works on isolated DNA. Formation of oxidatively generated lesions was also determined *in vitro*.

7.3.1 UVB and oxidative stress

Although often discussed for the effect of UVA, oxidatively generated DNA lesions are also relevant in the effects of UVB. The relative yield of this class of damage with respect to CPDs is yet very much in favour of the latter. For instance, the difference in yields of formamidopyrimidine glycosylase (Fpg)- and T4 endonuclease V (T4endoV)-sensitive sites, corresponding respectively to oxidized guanines and CPDS, is approximately 1000 in CHO cells in the 290-320 nm range [8]. Similar results were reported in human fibroblasts [47]. The underlying mechanisms, that may involve excitation of catalase [87], cyclooxygenase and reduced nicotinamide adenine dinucléotide phosphate (NADPH) [88, 89], remain to be fully elucidated. An interesting recent result, extensively discussed in the chapter 3 by D. Markovitsi in this volume, is the possible direct ionization triggered by absorption of UV photons by DNA bases, even below the energy corresponding to the ionization threshold [90-92].

7.3.2 Main UVA-induced photooxidation pathways

UVA is only poorly absorbed by DNA and does not provide enough energy to induce photoionization of DNA components. Therefore, all oxidation reactions induced in UVA-irradiated cells arise from photosensitized reactions. In these processes, UVA photons are absorbed by endogenous cellular components [93] that, upon excitation,

trigger oxidation reactions and release of oxidizing species. Numerous works on model systems and isolated DNA has provided valuable mechanistic information.

7.3.2.1 One-electron oxidation reactions

A first photosensitized process involves electron abstraction from DNA bases and is known as “type I photosensitization”. This photoreaction has been found to be efficient with all nucleic bases studied as isolated monomer when the oxidation potential of the excited photosensitizer is large enough. However, when taking place in double stranded DNA, one-electron oxidation leads to the sole formation of damage at guanine bases [94-96]. This is explained by the much lower ionization potential of this base compared to other DNA components. Consequently, radical cations produced on T, C or A migrate within DNA to guanine residues where the guanine radical cation gives rise to oxidation products. Those are mostly 8-oxoGua and 4-hydroxy-5-formamidopyrimidine (FapyGua). Secondary oxidation products of 8-oxoGua can be produced at large dose but not under biologically relevant condition.

7.2.3.2 Singlet oxygen

Rather than reacting with DNA components, photosensitizers in their excited state may transfer their energy to dioxygen. Unlike most molecules, the ground state of dioxygen is a triplet state, which limits its direct reactivity with DNA components. However, transfer of energy from the triplet excited state of the sensitizers converts it into the highly reactive singlet oxygen ($^1O_2$) in a “type II photosensitization reaction”. This species, that is not a radical, readily reacts with double bonds in organic molecules leading to the formation of endoperoxides and dioxetanes. It can also lead to the formation of hydroperoxide through the ene-reaction and oxidize sulphur atoms. In

DNA, only guanine reacts with $^1O_2$ with formation of an endoperoxide that further leads to the formation of 8-oxoGua as the only reaction product [94, 95, 97].

7.2.3.3 Reactive oxygen species arising from the superoxide anion radical

Superoxide anion ($O_2^{\bullet -}$) is produced in large amounts in UV-irradiated cells as the result of enzymatic process or by release from mitochondria [98]. Superoxide anion is poorly reactive with DNA but is at the origin of more damaging species. Upon dismutation, either catalysed by redox metals or performed by the superoxide dismutase enzymes, $O_2^{\bullet -}$ gives rise to hydrogen peroxide H_2O_2. Hydrogen peroxide is also unable to directly damage DNA. However, reduced metal ions like Fe^{2+} or Cu^{+} may convert it into the highly reactive hydroxyl radical •OH. In this reaction, metal ions are oxidized into Fe^{3+} or Cu^{2+}. The reducing environment of cells, mostly resulting from the large concentration in glutathione, allows the conversion of these ions back to their reduced forms able to react again with H_2O_2. This process is worsened by the release of iron from its storage proteins upon UVA irradiation [99, 100]. The high reactivity of •OH leads to the formation of a wide series of damage to the four DNA bases [99, 100]. Purines are converted into 8-oxo and formamidopyrimidine derivatives upon attack at the C8 position. •OH also reacts efficiently with the C5-C6 double bond of pyrimidines, and leads to the formation of 5,6-dihydroxy-5,6-dihydro derivatives (thymine and cytosine glycols) and 5-hydroxycytosine. Oxidation reactions also take place on the methyl group of thymine with formation of 5-hydroxymethyl- and 5-formyl- uracil. •OH can also perform hydrogen atom abstraction from the deoxyribose moiety of the sugar-phosphate backbone [99, 100]. Consequently, it is one of the few species that can induce DNA strand breaks. The superoxide anion not only leads to the formation reactive oxygen species but also of nitrogen oxidizing derivatives. The most documented

pathway involves its reaction with NO that leads to the formation of peroxynitrite HOONO and, after subsequent reaction with CO_2, of nitrosoperoxy carbonate $ONOOCO_2^-$. While the former compound damages DNA through its decomposition into •OH [101], the latter gives rise to carbonate radical anion that is a one-electron oxidant [102].

7.3.3. Oxidatively generated DNA damage in UVA-irradiated cells

Information on the formation of oxidation products in the DNA of UVA irradiated cells was mostly inferred from enzymatic assays associated with either electrophoretic analysis or alkaline elution. In these approaches treatment with purified DNA repair enzymes are added to the protocol in order to convert specific classes of DNA base damage into strands breaks that add to those directly produced by the irradiation. The most frequently used enzymes are bacterial Formamidopyrimidine glycosylase and Endonuclease III that recognize oxidized purines and oxidized pyrimidines, respectively. T4endoV allows the detection of CPDs. In all reported studies, oxidized purines, most likely 8-oxoGua, are produced in larger amounts than direct strand breaks over the entire UVA range [8, 103]. Additional works showed that oxidized pyrimidines are minor lesions [103]. The distribution of DNA oxidatively generated lesions in UVA-irradiated cells differs from that induced by the hydroxyl radicals produced by γ-rays and from that induced by singlet oxygen produced by a specific sensitizer. The ratio between the relative yield of direct strand breaks, Fpg-sensitive sites and Endo-III sensitive sites were 1/0.47/0.16, 0.37/1/0.4 and 1/0.25/0, respectively [103]. This observation, combined with the fact that type I photosensitization is believed to be only weakly involved in the formation of oxidatively generated DNA lesions [97], led to the conclusion that 80% of the DNA damaging oxidizing species are singlet oxygen and

20% hydroxyl radicals [103]. It should be stressed that the yield of oxidatively generated lesions is not the same in all cell types. For example, melanocytes are more sensitive than other cutaneous cells upon UVA irradiation as the result of the presence of photosensitizing pheomelanin [49, 104-107].

8-OxoGua being the most frequent oxidatively generated lesion, it can be used as a probe to compare oxidative stress and CPD formation in the UVA range. Using broadband sources and either enzymatic or chromatographic assays, CPDs have been detected in larger amounts in all cell types including CHO cells and human keratinocytes and melanocytes. The ratio between the amounts of CPD and 8-oxoGua is approximatively 5 [22, 46, 48], with the exception of melanocytes where the larger yield of 8-oxoGua leads to a ratio of 1.5 [49]. This ratio is yet wavelength-dependent as shown in CHO cells where the values are 10 at 340 nm, 5.5 at 365 nm and 1 at 390 nm [8]. It can thus be concluded from these series of results that oxidatively generated lesions cannot be considered as the most frequent damaging events of the nuclear DNA in UVA-irradiated cells. Of course, this does not rule out that oxidative stress exhibits major effects on other biomolecules and in other cell compartments.

7.4 Spectral composition and photoproduct distribution

Most of the data available on the DNA damaging of sunlight were obtained with pure UVB or UVA sources. Some more environmentally relevant works used simulated sunlight that gathered the effects of both spectral ranges. However, only limited amounts of information are available on the possible combined effects of different wavelength ranges. The photobiological responses may not be additive and lead to antagonistic or synergistic effects on the induction of some types of DNA damage. Occurrence of such phenomena would emphasize the need to take into account the emission spectra of the UV source. This is partially done when weighted action spectra

412 are used but this approach relies only on additivity. Evidence are already available in
413 field of DNA damage of such complex spectral effects [108].

414 ### 7.4.1 Formation of Dewar valence isomers

415 Dewar valence isomers [36] are produced when 64-PPs absorb a UV photon and
416 undergo an intramolecular electrocyclisation in their pyrimidone ring [37]. The latter
417 moiety exhibits a maximum absorption at 325 nm in TT and CT 64-PP and at 315 nm
418 in TC and CC 64-PP [38, 39, 109]. Consequently, UVB is expected to efficiently induce this
419 reaction. This is actually the case in model systems like small oligonucleotides but
420 much less in isolated and cellular double-stranded DNA, at least at biologically relevant
421 doses [12, 21]. This difference is explained by the overwhelming presence of normal
422 bases that preferentially absorb UVB photons, which are then not available for the
423 isomerization of 64-PPs [110]. Interestingly, 64-PPs exhibit a residual absorption in the
424 UVA range. The ratios between the areas under the curve of the absorption spectrum
425 in the UVB (240-320 nm) and UVA (320-380) are 0.76 for TT 64-PP and 0.44 for TC
426 64-PP. By comparison, the corresponding value is only 0.02 for DNA. These figures
427 shows the much lower shielding effect of 64-PP by normal DNA bases in the UVA than
428 the UVB range. This ability of UVA at photoisomerising 64-PPs was put forward already
429 in the first article reporting the structure of Dewar in dinucleoside monophosphate [38].
430 Since then, several works using different quantification tools have shown that Dewars
431 are present in significant amounts in cells exposed to simulated sunlight, namely a
432 combination of UVB and UVA [12, 46, 111, 112]. Additional support for the biological
433 relevance of Dewar isomer came from the observation of its formation in cells exposed
434 to natural sunlight [113, 114] and from its unambiguous detection in marine
435 microorganisms collected in the ocean [115]. Recently, the extent of photoisomerisation
436 of 64-PPs in isolated DNA exposed to sunlight was reported to depend on the season

[116], following the UVB/UVA ratio. It is difficult to provide a value for the ratio between the amount of 64-PPs and Dewars generated in DNA by exposure to natural or simulated sunlight. Indeed, the proportion of Dewars increases at the expense of that of 64-PPs when the dose increases. All these results could be rationalized in terms of emission spectrum and absorption at the different wavelengths [110].

7.4.2. UV-induced formation of sensitizers

Pyrimidine dimers are not the only types of photodamage impacted by the effects of two UV wavelengths ranges. Although this process has not been directly documented in cells, test tube experiments strongly suggest that UVB-mediated degradation of various biomolecules leads to the formation of photosensitizers that increase the extent of UVA-mediated oxidative stress. A first example are endogenously produced pterin derivatives [117, 118] . Pterin is a well-known photosensitizer studied for its damaging properties of biomolecules and its application in photodynamic therapy [119-121]. Another source of photosensitizing photoproducts is tryptophan. Its main photoproduct is N-formylkynurenine that is known to exhibit photodynamic properties [122, 123]. UVB irradiation of tryptophan also generates 6-formylindolo[3,2-b]carbazole (FICZ) which is also a photosensitizer [124]. The yield of FICZ is yet very low [125] and its role in UVA-induced oxidative stress is unlikely. Other combinations of wavelengths may enhance oxidative stress. For example, UVA-induced lipofuscin was reported to photosensitize keratinocytes to visible light [126].

7.4.3. Impact of UVA on the repair of UVB-induced dimers

Several works have unambiguously shown that exposure to UVB, especially in a chronic or repetitive pattern, led to the enhancement of DNA repair capacities [127-131] and in particular of nucleotide excision repair, which handles pyrimidine dimers.

Evidence are also accumulating that UVA exhibits the opposite effects. Exposure to UVA prior to UVB has been shown to reduce the rate of removal of CPDs, both in keratinocytes [9] and melanocytes [132]. *In vitro* studies also showed that UVA, alone or in the presence of photosensitizer, induced oxidative damage to repair proteins [133] like RPA [134] or PCNA [135]. The combination of these two opposite impacts of UVB and UVA on DNA repair strongly suggests that the persistence of pyrimidine dimers could depend on the ratio between these two wavelength ranges in the spectrum of the incident light.

7.5 DNA damage at the nucleotide resolution in cellular DNA

The advent of genome sequencing opens new avenues for the analysis of UV-induced pyrimidine dimers. In recent years, several techniques were developed for the identification and study of CPDs and 64-PPs at single-nucleotide resolution (Fig. 7.2). UV dimers have been mapped in bacteria [136], yeast [29, 137, 138], and human genomes [6, 28, 30, 31, 139]. Three major molecular approaches have been applied to pinpoint the damage positions. The first relies on damage-specific endonucleases to fragment DNA, and identifies damage sites based on the nucleotides at the fragment ends. CPD-seq, adduct-seq, and most recently GLOE-seq rely on the T4endoV and were therefore only applied to CPDs [29-31]. In contrast, excision-seq and UVDE-seq [137, 138] use the UV damage endonuclease (UVDE) and can map both CPDs and 64-PPs. However, this technique requires very high damage levels and has not been applied to mammalian genomes. The second approach, used by HS-Damage-seq [6], relies on blocking of DNA polymerases by the pyrimidine dimers. Here, damaged DNA from cells is subjected to *in vitro* primer extension, and the position of the lesion is identified again based on the fragment end. Using anti-CPD and anti-64-PP antibodies allows discrimination and mapping of the two damage types separately. The third and last approach is most

straightforward, but is so far limited in its application. This approach relies on identification of the damage-sites directly during single-molecule real-time (SMRT) sequencing. Pyrimidine dimers significantly block DNA polymerization and will alter polymerase kinetics. Direct sequencing of dimers was published in 2011 using synthetic oligonucleotides [140] and has not significantly advanced since, suggesting a difficulty of scaling to genomic sequences. The recent RADAR-seq method [136] may overcome these hurdles since it bypasses the necessity to directly sequence dimers: it uses T4 endonuclease IV to nick at damage site and *in vitro* synthesis to replace the dimer with a stretch of modified nucleotides prior to SMRT sequencing. However, RADAR-seq reduces the resolution of damage detection and has so far only been applied to *in vitro* irradiated bacterial DNA.

Analysis of the specific pyrimidines composing CPDs, performed with different methods, cell types, and UVC or UVB doses all showed a preference for TT>TC>CT>CC [6, 28-31]. HS-Damage-seq, excision-seq and UVDE-seq have also been used to map 64-PP in human and yeast genomes, and have found damages to form preferentially in TC>TT>CT>CC [6, 137, 138]. These preferences are consistent with the previous bulk DNA analyses. While UVDE will excise multiple photoproduct types, in UVDE-seq, UV-irradiated DNA was pre-treated with photolyase to remove CPDs. This allowed the identification of not only 64-PP but also non-canonical TA and AC photoproducts [138]. In addition to identifying the specific nucleotides composing the dimers, sequencing-based methods also provide the immediate sequence context of dimers. Thus, these methods show enrichment of CPD damage formation within T-tracks of DNA, and the preference for 64-PP damage formation in TC or TT sequences flanked by a C upstream and an A downstream of the damaged site [6, 137].

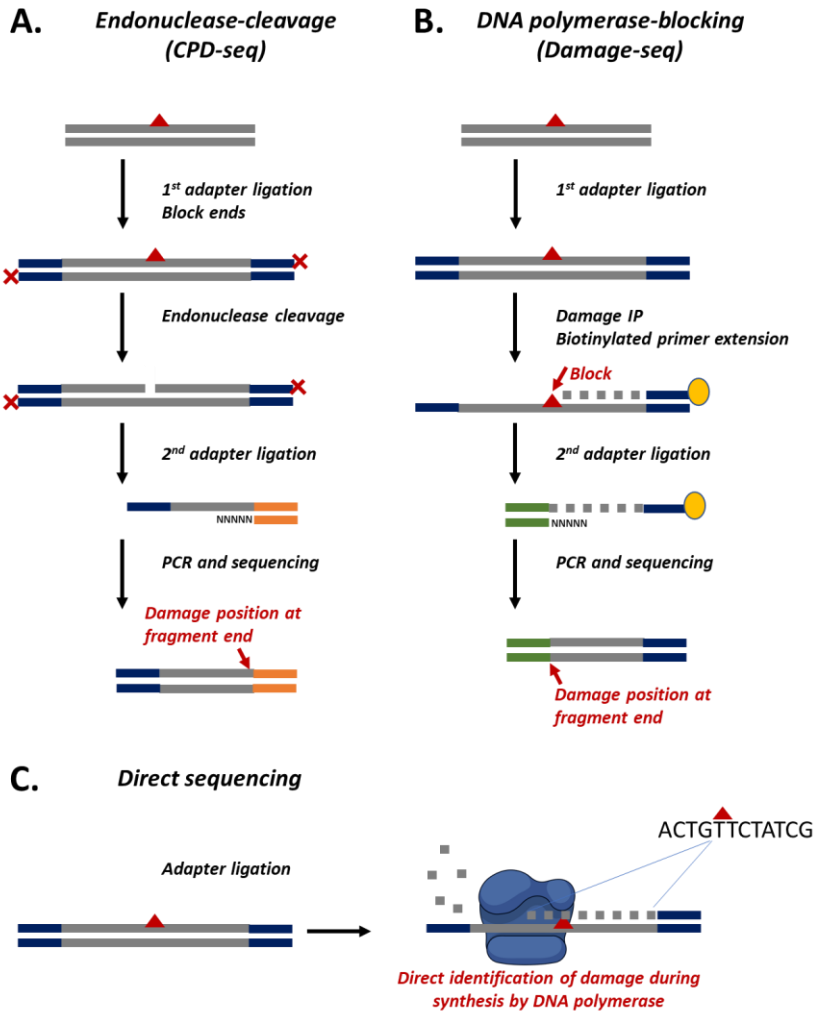

Figure 7.2. The three major approaches to mapping UV induced dimers. A) Mapping UV dimers based on endonuclease cleavage sites. Prior to cleavage free 3'-OH groups are blocked in order to obstruct adapter ligation. Shown is the schematic of CPD-seq. Adduct-seq, GLOE-seq, excision-seq and UVDE-seq are similar to CPD-seq but slightly modified. B) Mapping dimers based on the position at which a DNA polymerase is blocked in-vitro (Damage-seq). C) Direct detection of damages through SMRT sequencing. Red triangle: UV dimer. Red X: blocked DNA ends. Yellow circle: biotin. Figure generated with Biorender.com

In the large mammalian genomes, obtaining a quantitative high-resolution map of every damageable bipyrimidine site requires extremely high sequencing coverage. Most of the studies to date have not produced such high-coverage maps. Instead, in order to analyze the chromosomal context of damage formation, studies average damage densities over aggregated sequences. These include the study of damage

formation over transcription start sites of genes, well-positioned nucleosome dyads or transcription factor binding sites:

7.5.1 Damage formation in genes

In general, the major determinant of CPD damage formation is the frequency of pyrimidine dimers, primarily TT sequences. This frequency is not uniform in the genome, and specifically in genes. TT sequences are depleted near the transcription start sites of genes, and asymmetrically distributed between the transcribed and non-transcribed strands, resulting in overall lower damage levels on the transcribed strands of genes [141].

7.5.2 Damage formation in nucleosomal DNA

Nucleosome positions are generally associated with a depletion of TT pairs that could lead to lower levels of damage [142]. Analysis of CPD formation after normalizing to the underlying TT frequencies in yeast and human genomes has shown that the rotational setting of the DNA in the nucleosome affects CPD damage formation: a 10bp periodicity in CPDs is observed, with peaks in the outward facing rotational settings [29, 143]. Control experiments with genomic DNA irradiated *in vitro* did not produce this effect confirming that this periodicity is indeed a product of nucleosome binding. This increase in damage frequency at specific rotational settings within a nucleosome can be explained by the conformational changes in DNA that result in the adjacent pyrimidine bases assuming a favorable angle for dimer formation. This aspect is discussed by Gillet at al. in chapter 6 of this book.

7.5.3 Damage formation at transcription factor binding sites

Transcription factor binding sites were identified as sites of elevated UV mutagenesis in melanoma. Several studies assessed damage formation at transcription factor

binding sites, focusing on bipyrimidines contained within or adjacent to the consensus binding motifs. In yeast, Abf1 and Reb1 binding sites were associated with lower CPD frequencies [29]. In humans, some transcription factors were associated with reduced, while others with elevated damage frequencies [6, 144] . These altered damage frequencies were absent in irradiated naked DNA or at unbound motif-sites in cells, indicating they are a direct result of binding. Like in nucleosomes, binding can alter DNA confirmation and result in favorable or unfavorable angles for dimerization. Three independent studies identified ETS1 binding sites as hotspots for damage formation, that were associated with subsequent melanoma mutation hotspots [28, 30, 139] .

Higher mutation rates could be a result of higher damage, but could also be the product of lower repair efficiency. Indeed, a recent study suggests that it is primarily the lower repair efficiency at transcription factor- bound sites that promotes mutagenesis [144]. Repair of UV damages is extensively discussed by John J. Wyrick in chapter 12 of this volume. A key factor in untangling the relative contributions of damage formation versus repair will be to understand how damages affect protein binding in chromatin, including nucleosomes and transcription factors, a subject far less studied to date.

7.6 UV-induced DNA damage in skin

Most of the information discussed above were obtained in *in vitro* models. The amount of information in skin is less abundant, mostly because of limitation in sample size and technical issues. However, data obtained by immunological assays and in particular immunohistochemistry, and chromatographic techniques provided insight on the impact of the organization of the cutaneous tissues on the formation of photodamage. The vast majority of the information available concerns pyrimidine dimers. Their results show that the skin morphology drastically affects the level of DNA damage (Fig. 7.3).

It should also be stressed that eyes represent another target of solar UV. The formation and repair of CPDs have only been investigated recently [145-148].

7.6.1 Yield of lesions in skin

UVB and UVA induce the formation of CPDs in both keratinocytes and melanocytes in the same yield in skin [50]. Interestingly, the mean value of the yield of CPDs induced by UVB in DNA of the epidermis is lower than in culture of keratinocytes, which are the most frequent cell types in this skin compartment [22]. This can be first explained by the protective effect of the stratum corneum. An additional explanation is the shielding effect of the different layers of keratinocytes in the epidermis [112]. This effect is wavelength-dependent with a decrease in the CPDs yield per cell layer 15 faster at 260 nm than at 230. Determination of accurate quantitative data also showed that the yield of CPDs was roughly 2 and 4 orders of magnitude lower at 320 and 365 nm, respectively, compared to 290 nm in both dermis and epidermis [69]. In the same study, 64-PPs were found to be produced in a constant ratio from 260 to 310 nm, and then strongly decrease at higher wavelengths. In contrast to UVB, UVA is poorly absorbed by the stratum corneum and penetrates through the keratinocytes layers without significant attenuation. These observations explain why the ratio between the yield of CPD in the UVB and UVA ranges is lower in skin than in cultured cells [22, 24, 48]. It should be stressed that immunohistochemistry results showed that the level of UVA-induced CPDs was slightly higher in the basal layer than in layers located above. [149]. This suggested the occurrence of a reflexion of UVA takes place at the dermal-epidermal junction.

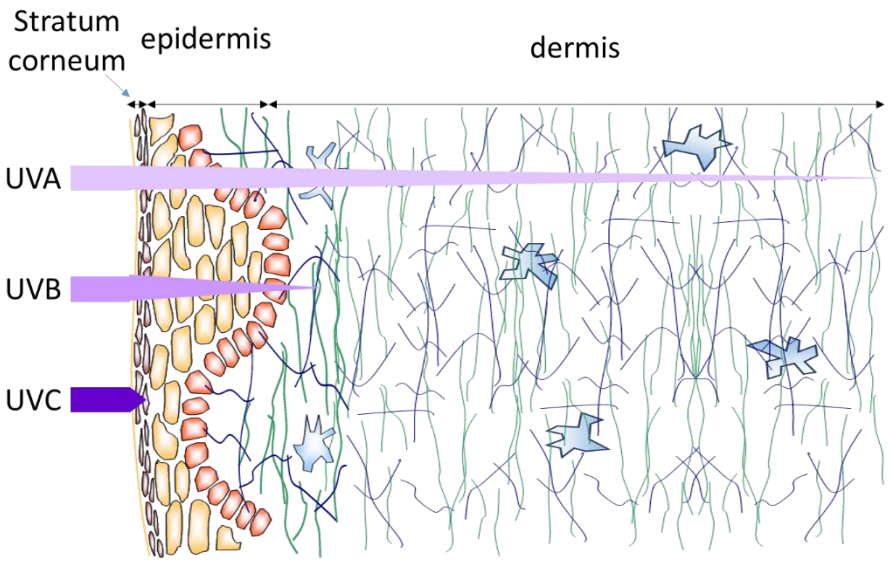

Figure 7.3: Penetration of UV radiation in human skin. The highly energetic UVC radiation are rapidly absorbed by the stratum corneum. UVB is absorbed in the epidermis and reaches the top of the dermis. In contrast, UVA is weakly attenuated and interacts with the whole dermis. In terms cell types, keratinocytes present in dense layers in the epidermis are much more affected by both UVA and UVB than fibroblasts sparsely spread in the dermal extracellular matrix.

7.6.2 Effect of phototype on the formation of CPDs

Phototypes is a convenient way to stratify the different skin types, which mostly reflect ethnic origins. In Caucasian, the risk of burning and the ability to tan upon exposure to sunlight has led to the definition of phototypes I (fair skin) to IV (brown skin). Phototypes V and VI are Asian and dark brown skins, respectively. A high skin phototype is known to be highly protective against skin cancer, as exemplified by studies carried out in areas harbouring fair- and dark-skinned populations [150-152]. On the average, protection factors of 20 and 70 against melanoma and carcinomas, respectively, were observed when skin of phototypes VI were compared to phototype II [153, 154]. This was only partially explained by the decrease in the mean level of CPD in keratinocytes that was found to be only 10-times lower in skin of phototype VI

compared to II following exposure to simulated sunlight or UVB [62, 155]. The same values were observed for both immediate and dark CPDs [62]. The latter result further suggests that photooxidation of melanin is not the only mechanism at the origin of dark CPDs. A better understanding of the impact of the phototype and of the melanin content was provided by experiments assessing the distribution of melanin and of the yield of CPDs. These works unambiguously showed that the best protection against CPDs between dark and fair skins was observed in basal layer, where the largest proportion of melanin is stored in dark skin [155-157]. The basal layer, that harbours the cells at the origin of melanomas and basal cell carcinomas, is much more protected than the rest of the epidermis. It should be stressed that these strong protective effects are no longer observed when less extreme phototypes are concerned. The ratio between the yield of CPDs in phototype II and IV is only approximately 1.5 [24, 158-160]. Another interesting data regarding pigmentation is that tanning of Caucasian skin affords only a weak protection of a factor 2 against the formation of CPDs [160-162].

7.7 Mutagenic consequences of DNA photodamage

The biological consequences of DNA photodamage in terms of carcinogenesis are mostly driven by their ability to induce mutations. A first requisite for a lesion to be mutagenic is that it escapes DNA repair as observed for pyrimidine dimers. The mutagenicity of a photodamage also depends on its chemical structure and the resulting impact on the coding properties upon replication of DNA. The combination of all the features explain the mutation spectra observed in tumours

7.7.1. *In vitro* data of UV-induced mutagenesis

UV-mutagenesis is investigated for years. The first works involved irradiation of plasmids further introduced and replicated in bacteria. These early studies showed that

UVB and UVC mostly led to mutation at bipyrimidine sites. The subsequent works took advantage of progress in oligonucleotide synthesis to study the specific mutational properties of individual pyrimidine dimers with purified polymerases or following incorporation in plasmids and replication in cells [163-167]. It was thus observed that TT CPD was poorly mutagenic in contrast to TT 64-PP mostly because of differences in impact of the lesions on the local structure of DNA. In contrast to TT CPD, deaminated TC CPD (TU CPD) were highly mutagenic, leading to C→T transitions because U codes like T during replication. The TC 64-PP was less mutagenic than the corresponding TT photoproduct [168]. In contrast, the TT Dewar was more mutagenic than the TC Dewar and less than the TT 64-PP. It is worth mentioning that in mammalian cells, in addition to deamination [41, 169] and structural modifications, mutagenesis of UV-induced photoproducts is largely explained by the role of translesional polymerases [170-172], as discussed in the chapter 16 by Menck et al. in this book. Some of these enzymes, like polymerase η, are referred to as “error-free” when bypassing pyrimidine dimers. They are thus expected to accurately incorporate A opposite T in TT CPDs, but also opposite U that would arise from C deamination in TC dimers. It should be stressed that experiments involving cells [20] or mice [173] transfected with specific repair enzymes led to the conclusion that these mutations mostly result from CPDs rather than 64-PPs, which are very efficiently repaired. Another important feature is that C→T transitions at TC sites are also predominant in cells exposed to UVA [45, 174, 175] in line with the predominant formation of CPDs in this wavelength range. The bulk of these data helped defining a UV mutational signature where C→T transition at TC sites and CC→TT tandem mutations were predominant [176, 177].

In vitro mutational data are also available for oxidatively generated damage. 8-OxoGua, following misincorporation of adenine upon replication leads to G→T

transversion [178]. Information were also obtained on the Fapy derivatives that show that FapyGua leads to G→T transversion while 4,6-Diamino-5-formamidopyrimidine (FapyAde) is poorly mutagenic [179]. Among thymine oxidation products, thymine glycols are strongly blocking lesions but poorly mutagenic. 5-Formyluracil also leads to a low mutation frequency [180]. In contrast, cytosine oxidation products are mutagenic, mostly following deamination [181, 182]. The contribution of these mutations to UVA-mutational signature is yet limited. The G→T transversion typical of the most frequent oxidatively generated lesions is a minor mutation, with the exception of one work involving mutation analyses in tumours collected in the basal layer [183]. Whole genome sequencing analysis of the mutation induced by UVA in xeroderma pigmentosum variant human cells failed to detect a significant contribution of oxidative damage but rather the mutation signature of pyrimidine dimers [184] with frequent mutations at bipyrimidine sites. Mutation at adenine is also observed [185] while adenine oxidation products are not frequent upon UVA irradiation.

7.7.2. Next generation sequencing of human tumours

Sequencing of specific genes in human tumours such as p53 has confirmed the presence of the UV signature [186-188]. The development of modern and fast sequencing techniques, which revolutionized the field of genomic, provided a novel and outstanding perspective on the mutations underlying human cancers. Next generation sequencing techniques have been used to determine millions of mutations present in thousands of tumours collected from different types of cancers [189, 190]. In the field of skin carcinogenesis, a first interesting result is that, together with lung cancers, melanoma is one of the cancer type accumulating the largest number of mutations per tumour [190-192]. The value is more than one order of magnitude larger than, for example, in leukaemia or medulloblastoma. This can be explained by the fact that skin is

constantly exposed to sunlight and accumulates numerous DNA damage and their resulting mutations during the development of the tumour. An interesting output of this sequencing effort is the statistical analysis of the databank that made possible the determination of mutational signatures [193, 194] available on-line from the COSMIC consortium [195]. Signatures bearing mutations at bipyrimidine sites (Table 7.2) are observed with a high frequency in melanoma [190, 196-199], basal cell carcinoma [200, 201], squamous cell carcinoma [202] and cutaneous T cell lymphoma [203]. They are basically absent from other cancer types. In the field of melanoma, the same approach allowed to show that acral and mucosal melanomas do not exhibit the same signature [197, 204]. Another interesting information provided by these techniques is related to a mutational signature associated with oxidative stress and 8-oxoGua. In the COSMIC database, this signature is observed in one third of the breast, prostate and stomach cancers but not in skin cancer. A last comment regarding melanoma is the high frequency of a A→T transversion leading to the *BRAF*^{V600E} mutation [205]. This mutation does not take place at a bipyrimidine site and does not correspond to known oxidative lesions. In addition, it is also frequent in a number of internal cancers and may thus not be of photobiological origin. However, recent UVDE-seq results in UVC-irradiated yeast proposed a role for AT dimers [138], although these photoproducts have been observed only in test tube experiments and in much lower yield than CPDs [206, 207].

Table 7.2: Proportion (in %) of different mutation signatures determined in the COSMIC database for skin cancers. Results represents the ratio between the number of tumours exhibiting each signature and the number total number of tumour of each cancer. BCC: basal cell carcinoma, SCC: squamous cell carcinoma.*

signature	7a	7b	7c	7d	tandem1	18
Mutations	C to T at TC	C-to T at TC and CC	T to A and T to C	T to C and C to T	CC to TT	oxydation
Melanoma	84	82	40	55	100	n.d.**
BCC	100	59	23	41	-	n.d.**

SCC	98	100	74	90	-	n.d.**

*: [195]

**: not detected

Abbreviations :

64-PP: Pyrimidine (6-4) pyrimidone photoproduct; 8-oxoGua: 8-oxo-7,8-dihydroguanine; BCC: basal cell carcinoma; CHO: Chinese hamster ovary cells; CPD: cyclobutane pyrimidine dimers; Dewar: Dewar valence isomer of 64-PP; FapyAde: 4,6-Diamino-5-formamidopyrimidine; FapyGua: 4-hydroxy-5-formamidopyrimidine; FICZ : 6-Formylindolo[3,2-b]carbazole; Fpg: formamidopyrimidine glycosylase; SAM S-adenosyl-methionine; SCC: squamous cell carcinoma; SMRT: single-molecule real-time sequencing; SP: spore photoproduct (5-(a-thyminyl)-thymine); T4endoV: endonuclease V of phage T4; UVDE: UV damage endonuclease

References

1. N. Kobayashi, S. Katsumi, K. Imoto, A. Nakagawa, S. Miyagawa, M. Furumura and T. Mori, *Pigment Cell Res.*, 2001, **14**, 94-102.
2. D. Mitchell and B. Brooks, *Photochem. Photobiol.*, 2010, **86**, 2-17.
3. G. P. Pfeifer, R. Drouin and G. P. Holmquist, *Mutat. Res.*, 1993, **288**, 39-46.
4. T. Douki, *Photochem. Photobiol. Sci.*, 2013, **12**, 1286-1302.
5. S. Adar, J. Hu, J. D. Lieb and A. Sancar, *Proc. Natl. Acad. Sci. USA*, 2016, **113**, E2124-2133.
6. J. Hu, O. Adebali, S. Adar and A. Sancar, *Proc. Natl. Acad. Sci. USA*, 2017, **114**, 6758-6763.
7. A. R. Collins, V. L. Dobson, M. Dusinska, G. Kennedy and R. Stetina, *Mutat. Res.*, 1997, **375**, 183-193.
8. C. Kielbassa, L. Roza and B. Epe, *Carcinogenesis*, 1997, **18**, 811-816.
9. S. Courdavault, C. Baudouin, M. Charveron, B. Canghilem, A. Favier, J. Cadet and T. Douki, *DNA Repair*, 2005, **4**, 836-844.
10. S. Courdavault, C. Baudouin, S. Sauvaigo, S. Mouret, S. Candéias, M. Charveron, A. Favier, J. Cadet and T. Douki, *Photochem. Photobiol.*, 2004, **79**, 145-151.
11. D. L. Mitchell, J. Jen and J. E. Cleaver, *Photochem. Photobiol.*, 1991, **54**, 741-746.
12. D. Perdiz, P. Grof, M. Mezzina, O. Nikaido, E. Moustacchi and E. Sage, *J. Biol. Chem.*, 2000, **275**, 26732-26742.
13. B. S. Rosenstein and D. L. Mitchell, *Photochem. Photobiol.*, 1987, **45**, 775-780.
14. J. E. Frederick, H. E. Snell and E. K. Haywood, *Photochem. Photobiol.*, 1989, **50**, 443-450.
15. C. Marionnet, C. Tricaud and F. Bernerd, *Int. J. Molec. Sci.*, 2015, **16**, 68-90.
16. A. J. Varghese, in *Photophysiology*, Academic Press, New-York, 1972, vol. 7, pp. 207-274.
17. S. Tommasi, M. F. Denissenko and G. P. Pfeifer, *Cancer Res.*, 1997, **57**, 4727-4730.
18. R. Drouin and J. P. Therrien, *Photochem. Photobiol.*, 1997, **66**, 719-726.
19. J.-H. Yoon, C.-S. Lee, T. R. O'Connor, A. Yasui and G. P. Pfeifer, *J. Mol. Biol.*, 2000, **299**, 681-693.
20. Y. H. You, D. H. Lee, J. H. Yoon, S. Nakajima, A. Yasui and G. P. Pfeifer, *J. Biol. Chem.*, 2001, **276**, 44688-44694.
21. T. Douki and J. Cadet, *Biochemistry*, 2001, **40**, 2495-2501.

22. S. Mouret, C. Baudouin, M. Charveron, A. Favier, J. Cadet and T. Douki, *Proc. Natl. Acad. Sci. USA*, 2006, **103**, 13765-13770.
23. P. J. Rochette, S. Lacoste, J. P. Therrien, N. Bastien, D. E. Brash and R. Drouin, *Mutat. Res.*, 2009, **665**, 7-13.
24. S. Mouret, M. T. Leccia, J. L. Bourrain, T. Douki and J. C. Beani, *J. Invest. Dermatol.*, 2011, **131**, 1539-1546.
25. N. Bastien, J. P. Therrien and R. Drouin, *Photochem. Photobiol. Sci.*, 2013, **12**, 1544-1554.
26. D. L. Mitchell, J. P. Allison and R. S. Nairn, *Radiat. Res.*, 1990, **123**, 299-303.
27. S. Mouret, M. Charveron, A. Favier, J. Cadet and T. Douki, *DNA Repair*, 2008, **7**, 704-712.
28. K. Elliott, M. Bostrom, S. Filges, M. Lindberg, J. Van den Eynden, A. Stahlberg, A. R. Clausen and E. Larsson, *Plos Genetics*, 2018, **14**.
29. P. Mao, M. J. Smerdon, S. A. Roberts and J. J. Wyrick, *Proc. Natl. Acad. Sci. USA*, 2016, **113**, 9057-9062.
30. S. Premi, L. Han, S. Mehta, J. Knight, D. J. Zhao, M. A. Palmatier, K. Kornacker and D. E. Brash, *Proc. Natl. Acad. Sci. USA*, 2019, **116**, 24196-24205.
31. A. M. Sriramachandran, G. Petrosino, M. Mendez-Lago, A. J. Schafer, L. S. Batista-Nascimento, N. Zilio and H. D. Ulrich, *Mol. Cell*, 2020, **78**, 975-+.
32. S. Matallana-Surget, J. A. Meador, F. Joux and T. Douki, *Photochem. Photobiol. Sci.*, 2008, **7**, 794-801.
33. L. Martinez-Fernandez, A. Banyasz, L. Esposito, D. Markovitsi and R. Improta, *Signal Transduct Target Ther*, 2017, **2**, 17021.
34. Y.-H. You and G. P. Pfeifer, *J. Mol. Biol.*, 1999, **293**, 493-503.
35. A. Banyasz, L. Esposito, T. Douki, M. Perron, C. Lepori, R. Improta and D. Markovitsi, *J. Phys. Chem. B*, 2016, **120**, 4232-4242.
36. T. Douki and E. Sage, *Photochem. Photobiol. Sci.*, 2015, **15**, 24-30.
37. K. Haiser, B. P. Fingerhut, K. Heil, A. Glas, T. T. Herzog, B. M. Pilles, W. J. Schreier, W. Zinth, R. de Vivie-Riedle and T. Carell, *Angew. Chem. Int. Ed.*, 2012, **51**, 408-411.
38. J.-S. Taylor and M. P. Cohrs, *J. Am. Chem. Soc.*, 1987, **109**, 2834-2835.
39. J.-S. Taylor, H.-L. Lu and J. J. Kotyk, *Photochem. Photobiol.*, 1990, **51**, 161-167.
40. Y. Barak, O. Cohen-fix and Z. Livneh, *J. Biol. Chem.*, 1995, **270**, 24174-24179.
41. L. A. Frederico, T. A. Kunkel and B. Ramsay Shaw, *Biochemistry*, 1990, **29**, 2532-2537.
42. I. Tessman, M. A. Kennedy and S. K. Liu, *J. Mol. Biol.*, 1994, **235**, 807-812.
43. J. C. Sutherland and K. P. Griffin, *Radiat. Res.*, 1981, **86**, 399-409.
44. R. M. Tyrrell, *Photochem. Photobiol.*, 1973, **17**, 69-73.
45. P. J. Rochette, J.-P. Therrien, R. Drouin, D. Perdiz, N. Bastien, E. A. Drobetsky and E. Sage, *Nucleic Acids Res.*, 2003, **31**, 2786-2794.
46. T. Douki, A. Reynaud-Angelin, J. Cadet and E. Sage, *Biochemistry*, 2003, **42**, 9221-9226.
47. E. Kvam and R. M. Tyrrell, *Carcinogenesis*, 1997, **18**, 2379-2384.
48. S. Courdavault, C. Baudouin, M. Charveron, A. Favier, J. Cadet and T. Douki, *Mutat. Res.*, 2004, **556**, 135-142.
49. S. Mouret, A. Forestier and T. Douki, *Photochem. Photobiol. Sci.*, 2012, **11**, 155-162.
50. A. R. Young, C. S. Potten, O. Nikaido, P. G. Parsons, J. Boenders, J. M. Ramsden and C. A. Chadmick, *J. Invest. Dermatol.*, 1998, **111**, 936-940.
51. F. E. Quaite, B. M. Sutherland and J. C. Sutherland, *Nature*, 1992, **358**, 576-578.
52. Z. Kuluncsics, D. Perdiz, E. Brulay, B. Muel and E. Sage, *J. Photochem. Photobiol. B: Biol.*, 1999, **49**, 71-80.
53. S. Mouret, C. Philippe, J. Gracia-Chantegrel, A. Banyasz, S. Karpati, D. Markovitsi and T. Douki *Org. Biomolec. Chem.*, 2010, **8**, 1706-1711.
54. Y. Jiang, M. Rabbi, M. Kim, C. H. Ke, W. Lee, R. L. Clark, P. A. Mieczkowski and P. E. Marszalek, *Biophys. J.*, 2009, **96**, 1151-1158.
55. A. Banyasz, T. Douki, R. Improta, T. Gustavsson, D. Onidas, I. Vaya, M. Perron and D. Markovitsi, *J. Am. Chem. Soc.*, 2012, **134**, 14834-14845.
56. S. Premi, S. Wallisch, C. M. Mano, A. B. Weiner, A. Bacchiocchi, K. Wakamatsu, E. J. Bechara, R. Halaban, T. Douki and D. E. Brash, *Science*, 2016, **347**, 842-847.
57. G. J. Delinasios, M. Karbaschi, M. S. Cooke and A. R. Young, *Sci. Rep.*, 2018, **8**.
58. W. Adam, C. R. Sahamoller and A. Schonberger, *J. Am. Chem. Soc.*, 1997, **119**, 719-723.
59. T. Douki, I. Berard, A. Wack and S. Andra, *Chem. Eur. J.*, 2014, **20**, 5787-5794.
60. A. A. Lamola, *Pure Appl. Chem.*, 1970, **24**, 599-610.
61. M. H. Patrick and J. M. Snow, *Photochem. Photobiol.*, 1977, **25**, 373-384.

62. D. Fajuyigbe, T. Douki, A. van Dijk, R. P. E. Sarkany and A. R. Young, *Pigment Cell Melanoma Res.*, 2020.
63. K. P. Lawrence, T. Douki, R. P. E. Sarkany, S. Acker, B. Herzog and A. R. Young, *Sci. Rep.*, 2018, **8**, 12722.
64. Y. Kebbi, A. I. Muhammad, A. S. Sant'Ana, L. do Prado-Silva, D. H. Liu and T. Ding, *Compr Rev Food Sci F*, 2020, **19**, 3501-3527.
65. M. Luckiesh and A. H. Taylor, *J Opt Soc Am*, 1946, **36**, 227-234.
66. E. a. E. R. SCHEER (Scientific Committee on Health, *Opinion on biological effects of UV-C radiation relevant to health with particular reference to UV-C lamps*, European Commission, 2017.
67. T. Fukui, T. Niikura, T. Oda, Y. Kumabe, H. Ohashi, M. Sasaki, T. Igarashi, M. Kunisada, N. Yamano, K. Oel, T. Matsumoto, T. Matsushita, S. Hayashi, C. Nishigori and R. Kuroda, *Plos One*, 2020, **15**.
68. S. Y. Wang, in *Photochemistry and Photobiology of Nucleic Acids*, Academic Press, New-York, 1976, vol. 1, pp. 295-356.
69. H. Ikehata, T. Mori, Y. Kamei, T. Douki, J. Cadet and M. Yamamoto, *Photochem. Photobiol.*, 2020, **96**, 94-104.
70. F. R. de Gruijl, *Eur. J. Cancer*, 1999, **35**, 2003-2009.
71. H. E. Johns, S. A. Rapaport and M. Delbück, *J. Mol. Biol.*, 1962, **4**, 104-114.
72. D. G. E. Lemaire and B. P. Ruzsicska, *Photochem. Photobiol.*, 1993, **57**, 755-769.
73. T. Douki, M. Court, S. Sauvaigo, F. Odin and J. Cadet, *J. Biol. Chem.*, 2000, **275**, 11678-11685.
74. T. Matsunaga, K. Hieda and O. Nikaido, *Photochem Photobiol*, 1991, **54**, 403-410.
75. N. Yamano, M. Kunisada, S. Kaidzu, K. Sugihara, A. Nishiaki-Sawada, H. Ohashi, A. Yoshioka, T. Igarashi, A. Ohira, M. Tanito and C. Nishigori, *Photochem. Photobiol.*, 2020, **96**, 853-862.
76. T. Melvin, S. Cunniffe, D. Papworth, T. Roldanarjona and P. O'Neill, *Photochem. Photobiol.*, 1997, **65**, 660-665.
77. T. Melvin, S. M. T. Cunniffe, P. O'Neill, A. W. Parker and T. RoldanArjona, *Nucleic Acids Res.*, 1998, **26**, 4935-4942.
78. J. E. Donnellan and R. B. Setlow, *Science*, 1965, **149**, 308-310.
79. W. L. Nicholson, B. Setlow and P. Setlow, *Proc. Natl. Acad. Sci. USA*, 1991, **88**, 8288-8292.
80. W. L. Nicholson, B. Setlow and P. Setlow, *Astrobiology*, 2002, **2**, 417-425.
81. A. Frances-Monerris, C. Hognon, T. Douki and A. Monari, *Chem. Eur. J.*, 2020, **26**, 14236-14241.
82. T. Douki, B. Setlow and P. Setlow, *Photochem. Photobiol. Sci.*, 2005, **4**, 951-957.
83. B. Setlow and P. Setlow, *Appl. Environ. Microbiol.*, 1993, **59**, 640-643.
84. C. Lindberg and G. Horneck, *J. Photochem. Photobiol. B-Biol.*, 1991, **11**, 69-80.
85. W. Taylor, E. Camilleri, D. L. Craft, G. Korza, M. Rocha Granados, J. Peterson, R. Szczpaniak, S. K. Weller, R. Moeller, T. Douki, W. W. K. Mok and P. Setlow, *Appl Environ Microbiol*, 2020, **86**, e03039-03019.
86. O. Berteau and A. Benjdia, *Photochem. Photobiol.*, 2017, **93**, 67-77.
87. M. Horikawa-Miura, N. Matsuda, M. Yoshida, Y. Okumura, T. Mori and M. Watanabe, *Radiat. Res.*, 2007, **167**, 655-662.
88. S. M. Beak, Y. S. Lee and J. A. Kim, *Biochimie*, 2004, **86**, 425-429.
89. H. Wang and I. E. Kochevar, *Free Radic. Biol. Med.*, 2005, **38**, 890-897.
90. A. Banyasz, T. Kelola, L. Martinez-Fernandez, R. Improta and D. Markovitsi, *Faraday Discussions*, 2018, **207**, 181-197.
91. A. Banyasz, L. martinez-Fernandez, C. Balty, M. Perron, T. Douki , R. Improta and D. Markovitsi, *J. Am. Chem. Soc.*, 2017, **139**, 10561-10568.
92. M. Gomez-Mendoza, A. Banyasz, T. Douki, D. Markovitsi and J. L. Ravanat, *J. Phys. Chem. Lett.*, 2016, **7**, 3945-3948.
93. G. T. Wondrak, M. K. Jacobson and E. L. Jacobson, *Photochem. Photobiol. Sci.*, 2006, **5**, 215-237.
94. J. Cadet and T. Douki, *Photochem. Photobiol. Sci.*, 2018, **17**, 1816-1841.
95. J. Cadet, A. Grand and T. Douki, in *Photoinduced Phenomena in Nucleic Acids Ii: DNA Fragments and Phenomenological Aspects*, eds. M. Barbatti, A. C. Borin and S. Ullrich, Springer-Verlag Berlin, Berlin, 2015, vol. 356, pp. 249-275.
96. J. Cadet, T. Douki and J. L. Ravanat, *Accounts Chem. Res.*, 2008, **41**, 1075-1083.
97. P. Di Mascio, G. R. Martinez, S. Miyamoto, G. E. Ronsein, M. H. G. Medeiros and J. Cadet, *Chem. Rev.*, 2019, **119**, 2043-2086.

98. R. Gniadecki, T. Thorn, J. Vicanova, A. B. Petersen and H. C. Wulf, *J. Cell. Biochem.*, 2000, **80**, 216-222.
99. A. Aroun, J. L. Zhong, R. M. Tyrrell and C. Pourzand, *Photochem. Photobiol. Sci.*, 2012, **11**, 118-134.
100. C. Pourzand, R. D. Watkin, J. E. Brown and R. M. Tyrrell, *Proc. Natl. Acad. Sci. USA*, 1999, **96**, 6751-6756.
101. L. J. Kennedy, K. Moore, J. L. Caulfield, S. R. Tannenbaum and P. C. Dedon, *Chem. Res. Toxicol.*, 1997, **10**, 386-392.
102. Y. A. Lee, B. H. Yun, S. K. Kim, Y. Margolin, P. C. Dedon, N. E. Geacintov and V. Shafirovich, *Chemistry*, 2007, **13**, 4571-4581.
103. J.-P. Pouget, T. Douki , M.-J. Richard and J. Cadet, *Chem. Res. Toxicol.*, 2000, **13**, 541-549.
104. E. Kvam and R. M. Tyrrell, *J. Invest. Dermatol.*, 1999, **113**, 209-213.
105. H. T. Wang, B. Choi and M. S. Tang, *Proc. Natl. Acad. Sci. USA*, 2010, **107**, 12180-12185.
106. E. Wenczl, G. P. van der Schans, L. Roza, R. Kolb, N. Smit and A. A. Schothorst, *J. Invest. Dermatol.*, 1998, **110**, 693-693.
107. E. Wenczl, G. P. Van der Schans, L. Roza, R. M. Kolb, A. J. Timmerman, N. P. Smit, S. Pavel and A. A. Schothorst, *J. Invest. Dermatol.*, 1998, **111**, 678-682.
108. T. Douki, *Photochem Photobiol*, 2020, **96**, 962-972.
109. T. Douki, L. Voituriez and J. Cadet, *Photochem. Photobiol.*, 1991, **27**, 293-297.
110. T. Douki, *Photochem. Photobiol.*, 2016, **92**, 587-594.
111. D. Bacqueville, T. Douki, L. Duprat, S. Rebelo-Moreira, B. Guiraud, H. Dromigny, V. Perier, S. Bessou-Touya and H. Duplan, *J. Photochem. Photobiol. B: Biol.*, 2015, **151**, 31-38.
112. C. A. Chadwick, C. S. Potten, O. Nikaido, T. Matsunaga, C. Proby and A. R. Young, *J. Photochem. Photobiol. B: Biol.*, 1995, **28**, 163-170.
113. P. H. Clingen, C. F. Arlett, L. Roza, T. Mori, O. Nikaido and M. H. L. Green, *Cancer Res.*, 1995, **55**, 2245-2248.
114. X. S. Qin, S. M. Zhang, M. Zarkovic, Y. Nakatsuru, S. Shimizu, Y. Yamazaki, H. Oda, O. Nikaido and T. Ishikawa, *Japanese Journal of Cancer Research*, 1996, **87**, 685-690.
115. J. A. Meador, A. J. Baldwin, J. D. Pakulski, W. H. Jeffrey, D. L. Mitchell and T. Douki, *Environm. Microbiol.*, 2014, **16**, 1808-1820.
116. K. Nishimura, H. Ikehata, T. Douki, J. Cadet, S. Sugiura and T. Mori, *Photochem. Photobiol.*, 2020, **in press**.
117. G. Cremer-Bartels and I. Ebels, *Proc. Natl. Acad. Sci. USA*, 1980, **77**, 2415-2418.
118. H. Rokos, W. D. Beazley and K. U. Schallreuter, *Biochem. Biophys. Res. Com.*, 2002, **292**, 805-811.
119. M. P. Serrano, C. Lorente, C. D. Borsarelli and A. H. Thomas, *Chemphyschem*, 2015, **16**, 2244-2252.
120. M. P. Serrano, M. Vignoni, C. Lorente, P. Vicendo, E. Oliveros and A. H. Thomas, *Free Radic. Biol. Med.*, 2016, **96**, 418-431.
121. H. Yamada, T. Arai, N. Endo, K. Yamashita, M. Nonogawa, K. Makino, K. Fukuda, M. Sasada and T. Uchiyama, *Biochem. Biophys. Res. Com.*, 2005, **333**, 763-767.
122. T. M. Dreaden, J. Chen, S. Rexroth and B. A. Barry, *J. Biol. Chem.*, 2011, **286**, 22632-22641.
123. P. Walrant and R. Santus, *Photochem. Photobiol.*, 1974, **19**, 411-417.
124. S. L. Park, R. Justiniano, J. D. Williams, C. M. Cabello, S. Qiao and G. T. Wondrak, *J. Invest. Dermatol.*, 2015, **135**, 1649-1658.
125. A. Youssef, A. von Koschembahr, S. Caillat, S. Corre, M. D. Galibert and T. Douki, *Photochem. Photobiol.*, 2018.
126. P. N. Tonolli, O. Chiarelli-Neto, C. Santacruz-Perez, H. C. Junqueira, I. S. Watanabe, F. G. Ravagnani, W. K. Martins and M. S. Baptista, *J. Invest. Dermatol.*, 2017, **137**, 2447-2450.
127. N. Chouinard, J. P. Therrien, D. L. Mitchell, M. Robert, R. Drouin and M. Rouabhia, *Biochemistry and Cell Biology-Biochimie Et Biologie Cellulaire*, 2001, **79**, 507-515.
128. D. L. Mitchell, R. Greinert, F. R. de Gruijl, K. L. H. Guikers, E. W. Breitbart, M. Byrom, M. M. Gallmeier, M. G. Lowery and B. Volkmer, *Cancer Res.*, 1999, **59**, 2875-2884.
129. R. Berube, M. C. Drigeard Desgarnier, T. Douki, A. Lechasseur and P. J. Rochette, *J. Invest. Dermatol.*, 2018, **138**, 405-412.
130. M. C. Drigeard Desgarnier, F. Fournier, A. Droit and P. J. Rochette, *PLoS One*, 2017, **12**, e0173740.
131. M. C. Drigeard Desgarnier and P. J. Rochette, *DNA Repair*, 2018, **63**, 56-62.
132. S. Kimeswenger, R. Dingelmaier-Hovorka, D. Foedinger and C. Jantschitsch, *Exp. Dermatol.*, 2018, **27**, 276-279.

133. P. Karran and R. Brem, *DNA Repair*, 2016, **44**, 178-185.
134. M. Guven, R. Brem, P. Macpherson, M. Peacock and P. Karran, *J. Invest. Dermatol.*, 2015, **135**, 2834-2841.
135. B. Montaner, P. O'Donovan, O. Reelfs, C. M. Perrett, X. Zhang, Y. Z. Xu, X. Ren, P. Macpherson, D. Frith and P. Karran, *EMBO Rep.*, 2007, **8**, 1074-1079.
136. K. M. Zatopek, V. Potapov, L. L. Maduzia, E. Alpaslan, L. X. Chen, T. C. Evans, J. L. Ong, L. M. Ettwiller and A. F. Gardner, *DNA Repair*, 2019, **80**, 36-44.
137. D. S. Bryan, M. Ransom, B. Adane, K. York and J. R. Hesselberth, *Genome Research*, 2014, **24**, 1534-1542.
138. M. F. Laughery, A. J. Brown, K. A. Bohm, S. Sivapragasam, H. S. Morris, M. Tchmola, A. D. Washington, D. Mitchell, S. Mather, E. P. Malc, P. A. Mieczkowski, S. A. Roberts and J. J. Wyrick, *Cell Rep*, 2020, **33**, 108401.
139. P. Mao, A. J. Brown, S. Esaki, S. Lockwood, G. M. K. Poon, M. J. Smerdon, S. A. Roberts and J. J. Wyrick, *Nature Comm.*, 2018, **9**.
140. T. A. Clark, K. E. Spittle, S. W. Turner and J. Korlach, *Genome Integr*, 2011, **2**, 10.
141. E. E. Heilbrun, M. Merav and S. Adar, *NAR Genom Bioinform*, 2021, **3**, lqab020.
142. A. Valouev, S. M. Johnson, S. D. Boyd, C. L. Smith, A. Z. Fire and A. Sidow, *Nature*, 2011, **474**, 516-520.
143. A. J. Brown, P. Mao, M. J. Smerdon, J. J. Wyrick and S. A. Roberts, *PLoS Genet*, 2018, **14**, e1007823.
144. J. Frigola, R. Sabarinathan, A. Gonzalez-Perez and N. Lopez-Bigas, *Nucleic Acids Res*, 2021, **49**, 891-901.
145. J. D. Mallet, M. M. Dorr, M. C. D. Desgarnier, N. Bastien, S. P. Gendron and P. J. Rochette, *Plos One*, 2016, **11**.
146. R. Mesa and S. Bassnett, *Investigative Ophthalmology & Visual Science*, 2013, **54**, 6789-6797.
147. J. D. Mallet and P. J. Rochette, *Photochem. Photobiol. Sci.*, 2013, **12**, 1310-1318.
148. J. D. Mallet and P. J. Rochette, *Photochem. Photobiol.*, 2011, **87**, 1363-1368.
149. A. Tewari, M. M. Grage, G. I. Harrison, R. Sarkany and A. R. Young, *Photochem. Photobiol. Sci.*, 2013, **12**, 95-103.
150. S. Del Bino and F. Bernerd, *Br. J. Dermatol.*, 2013, **169**, 33-40.
151. D. Fajuyigbe and A. R. Young, *Pigment Cell Melanoma Res.*, 2016, **29**, 607-618.
152. S. Del Bino, C. Duval and F. Bernerd, *Int J Mol Sci*, 2018, **19**.
153. T. Hore, E. Robinson and R. C. W. Martin, *World J. Surg.*, 2010, **34**, 1788-1792.
154. M. Norval, P. Kellett and C. Y. Wright, *Photodermatol. Photoimmunol. Photomed.*, 2014, **30**, 262-265.
155. S. Del Bino, J. Sok and F. Bernerd, *British J. Dermatol.*, 2013, **168**, 1120-1123.
156. D. Fajuyigbe, S. M. Lwin, B. L. Diffey, R. Baker, D. J. Tobin, R. P. E. Sarkany and A. R. Young, *FASEB J.*, 2018, fj201701472R.
157. F. Rijken, P. L. Bruijnzeel, H. van Weelden and R. C. Kiekens, *J Invest Dermatol*, 2004, **122**, 1448-1455.
158. T. Gambichler, G. Moussa, N. S. Tomi, V. Paech, P. Altmeyer and A. Kreuter, *Photochem. Photobiol.*, 2006, **82**, 1097-1102.
159. J. M. McGregor, C. A. Harwood, L. Brooks, S. A. Fisher, D. A. Kelly, J. O'Nions, A. R. Young, T. Surentheran, J. Breuer, T. P. Millard, C. M. Lewis, I. M. Leigh, A. Storey and T. Crook, *J. Invest. Dermatol.*, 2002, **119**, 84-90.
160. A. R. Young, C. S. Potten, C. A. Chadwick, G. M. Murphy, J. L. Hawk and A. J. Cohen, *J. Invest. Dermatol.*, 1991, **97**, 942-948.
161. J. M. Sheehan, N. Cragg, C. A. Chadwick, C. S. Potten and A. R. Young, *J. Invest. Dermatol.*, 2002, **118**, 825-829.
162. J. M. Sheehan, C. S. Potten and A. R. Young, *Photochem. Photobiol.*, 1998, **68**, 588-592.
163. J.-S. Taylor and C. L. O'Day, *Biochemistry*, 1990, **29**, 1624-1632.
164. M. J. Horsfall and C. W. Lawrence, *J. Mol. Biol.*, 1993, **235**, 465-471.
165. N. Jiang and J.-S. Taylor, *Biochemistry*, 1993, **32**, 472-481.
166. C. W. Lawrence, P. E. M. Gibbs, A. Borden, M. J. Horsfall and B. J. Kilbey, *Mutat. Res.*, 1993, **299**, 157-163.
167. J.-S. Taylor, *Acc. Chem. Res.*, 1994, **27**, 76-82.
168. J. E. LeClerc, A. Borden and C. W. Lawrence, *Proc. Natl. Acad. Sci. USA*, 1991, **88**, 9685-9689.
169. W. Peng and B. R. Shaw, *Biochemistry*, 1996, **35**, 10172-10181.
170. H. Ikehata and T. Ono, *J. Radiat. Res.*, 2011, **52**, 115-125.
171. N. M. Makridakis and J. K. Reichardt, *Frontiers in Genetics*, 2012, **3**, 174.

172. A. Quinet, D. J. Martins, A. T. Vessoni, D. Biard, A. Sarasin, A. Stary and C. F. Menck, *Nucleic Acids Res*, 2016, **44**, 5717-5731.
173. J. Jans, W. Schul, Y. G. Sert, Y. Rijksen, H. Rebel, A. P. Eker, S. Nakajima, H. van Steeg, F. R. de Gruijl, A. Yasui, J. H. Hoeijmakers and G. T. van der Horst, *Curr. Biol.*, 2005, **15**, 105-115.
174. U. P. Kappes, D. Luo, M. Potter, K. Schulmeister and T. M. Rünger, *J. Invest. Dermatol.*, 2006, **126**, 667-675.
175. H. Ikehata, K. Kawai, J. Komura, K. Sakatsume, L. C. Wang, M. Imai, S. Higashi, O. Nikaido, K. Yamamoto, K. Hieda, M. Watanabe, H. Kasai and T. Ono, *J. Invest. Dermatol.*, 2008, **128**, 2289-2296.
176. D. E. Brash, *Photochem. Photobiol.*, 2015, **91**, 15-26.
177. E. Sage, P. M. Girard and S. Francesconi, *Photochem. Photobiol. Sci.*, 2012, **11**, 74-80.
178. X. Z. Tan, A. P. Grollman and S. Shibutani, *Carcinogenesis*, 1999, **20**, 2287-2292.
179. M. A. Kalam, K. Haraguchi, S. Chandani, E. L. Loechler, M. Moriya, M. M. Greenberg and A. K. Basu, *Nucleic Acids Res.*, 2006, **34**, 2305-2315.
180. H. Kamiya, N. Murata-Kamiya, N. Karino, Y. Ueno, A. Matsuda and H. Kasai, *Mutat. Res.*, 2002, **513**, 213-222.
181. D. A. Kreutzer and J. M. Essigmann, *Proc. Natl. Acad. Sci. USA*, 1998, **95**, 3578-3582.
182. A. A. Purmal, Y. W. Kow and S. S. Wallace, *Nucleic Acids Res.*, 1994, **22**, 72-78.
183. N. S. Agar, G. M. Halliday, E. S. C. Barnetson, H. N. Ananthaswamy, M. Wheeler and A. M. Jones, *Proc. Natl. Acad. Sci. USA*, 2004, **101**, 4954-4959.
184. N. C. Moreno, T. A. de Souza, C. C. M. Garcia, N. Q. Ruiz, C. Corradi, L. P. Castro, V. Munford, S. Ienne, L. B. Alexandrov and C. F. M. Menck, *Nucleic Acids Res*, 2020, **48**, 1941-1953.
185. E. Sage, B. Lamolet, E. Brulay, E. Moustacchi, A. Chateauneuf and E. A. Drobetsky, *Proc. Natl. Acad. Sci. USA*, 1996, **93**, 176-180.
186. D. E. Brash, J. A. Rudolph, J. A. Simon, A. Lin, G. J. McKenna, H. P. Baden, A. J. Halperin and J. Ponten, *Proc. Natl. Acad. Sci. U.S.A.*, 1991, **88**, 10124-10128.
187. N. Dumaz, C. Drougard, A. Sarasin and A. L. Daya-Grosjean, *Proc. Natl. Acad. Sci. USA*, 1993, **90**, 10529-10533.
188. A. Ziegler, D. J. Leffel, S. Kunala, H. W. Sharma, P. E. Shapiro, A. E. Bale and D. E. Brash, *Proc. Natl. Acad. Sci. U.S.A.*, 1993, **90**, 4216-4220.
189. L. B. Alexandrov, J. Kim, N. J. Haradhvala, M. N. Huang, A. W. Tian Ng, Y. Wu, A. Boot, K. R. Covington, D. A. Gordenin, E. N. Bergstrom, S. M. A. Islam, N. Lopez-Bigas, L. J. Klimczak, J. R. McPherson, S. Morganella, R. Sabarinathan, D. A. Wheeler, V. Mustonen, P. M. S. W. Group, G. Getz, S. G. Rozen, M. R. Stratton and P. Consortium, *Nature*, 2020, **578**, 94-101.
190. L. B. Alexandrov, S. Nik-Zainal, D. C. Wedge, S. A. J. R. Aparicio, S. Behjati, A. V. Biankin, G. R. Bignell, N. Bolli, A. Borg, A. L. Borresen-Dale, S. Boyault, B. Burkhardt, A. P. Butler, C. Caldas, H. R. Davies, C. Desmedt, R. Eils, J. E. Eyfjord, J. A. Foekens, M. Greaves, F. Hosoda, B. Hutter, T. Ilicic, S. Imbeaud, M. Imielinsk, N. Jager, D. T. W. Jones, D. Jones, S. Knappskog, M. Kool, S. R. Lakhani, C. Lopez-Otin, S. Martin, N. C. Munshi, H. Nakamura, P. A. Northcott, M. Pajic, E. Papaemmanuil, A. Paradiso, J. V. Pearson, X. S. Puente, K. Raine, M. Ramakrishna, A. L. Richardson, J. Richter, P. Rosenstiel, M. Schlesner, T. N. Schumacher, P. N. Span, J. W. Teague, Y. Totoki, A. N. J. Tutt, R. Valdes-Mas, M. M. van Buuren, L. van 't Veer, A. Vincent-Salomon, N. Waddell, L. R. Yates, J. Zucman-Rossi, P. A. Futreal, U. McDermott, P. Lichter, M. Meyerson, S. M. Grimmond, R. Siebert, E. Campo, T. Shibata, S. M. Pfister, P. J. Campbell, M. R. Stratton, A. P. C. Genome, I. B. C. Consortium, I. M.-S. Consortium and I. PedBrain, *Nature*, 2013, **500**, 415-421.
191. C. Greenman, P. Stephens, R. Smith, G. L. Dalgliesh, C. Hunter, G. Bignell, H. Davies, J. Teague, A. Butler, C. Stevens, S. Edkins, S. O'Meara, I. Vastrik, E. E. Schmidt, T. Avis, S. Barthorpe, G. Bhamra, G. Buck, B. Choudhury, J. Clements, J. Cole, E. Dicks, S. Forbes, K. Gray, K. Halliday, R. Harrison, K. Hills, J. Hinton, A. Jenkinson, D. Jones, A. Menzies, T. Mironenko, J. Perry, K. Raine, D. Richardson, R. Shepherd, A. Small, C. Tofts, J. Varian, T. Webb, S. West, S. Widaa, A. Yates, D. P. Cahill, D. N. Louis, P. Goldstraw, A. G. Nicholson, F. Brasseur, L. Looijenga, B. L. Weber, Y. E. Chiew, A. DeFazio, M. F. Greaves, A. R. Green, P. Campbell, E. Birney, D. F. Easton, G. Chenevix-Trench, M. H. Tan, S. K. Khoo, B. T. Teh, S. T. Yuen, S. Y. Leung, R. Wooster, P. A. Futreal and M. R. Stratton, *Nature*, 2007, **446**, 153-158.
192. B. Vogelstein, N. Papadopoulos, V. E. Velculescu, S. B. Zhou, L. A. Diaz and K. W. Kinzler, *Science*, 2013, **339**, 1546-1558.
193. L. B. Alexandrov, S. Nik-Zainal, D. C. Wedge, P. J. Campbell and M. R. Stratton, *Cell Rep.*, 2013, **3**, 246-259.
194. M. Petljak and L. B. Alexandrov, *Carcinogenesis*, 2016, **37**, 531-540.

195. C. consortium, 2020.
196. S. Haghdoost, L. Sjolander, S. Czene and M. Hanns-Ringdahl, *Free Radic. Biol. Med.*, 2006, **41**, 620-626.
197. E. Hodis, I. R. Watson, G. V. Kryukov, S. T. Arold, M. Imielinski, J. P. Theurillat, E. Nickerson, D. Auclair, L. R. Li, C. Place, D. DiCara, A. H. Ramos, M. S. Lawrence, K. Cibulskis, A. Sivachenko, D. Voet, G. Saksena, N. Stransky, R. C. Onofrio, W. Winckler, K. Ardlie, N. Wagle, J. Wargo, K. Chong, D. L. Morton, K. Stemke-Hale, G. Chen, M. Noble, M. Meyerson, J. E. Ladbury, M. A. Davies, J. E. Gershenwald, S. N. Wagner, D. S. B. Hoon, D. Schadendorf, E. S. Lander, S. B. Gabriel, G. Getz, L. A. Garraway and L. Chin, *Cell*, 2012, **150**, 251-263.
198. L. D. Trucco, P. A. Mundra, K. Hogan, P. Garcia-Martinez, A. Viros, A. K. Mandal, N. Macagno, C. Gaudy-Marqueste, D. Allan, F. Baenke, M. Cook, C. McManus, B. Sanchez-Laorden, N. Dhomen and R. Marais, *Nature Med.*, 2019, **25**, 350-350.
199. J. S. Wilmott, P. A. Johansson, F. Newell, N. Waddell, P. Ferguson, C. Quek, A. M. Patch, K. Nones, P. Shang, A. L. Pritchard, S. Kazakoff, O. Holmes, C. Leonard, S. Wood, Q. Xu, R. P. M. Saw, A. J. Spillane, J. R. Stretch, K. F. Shannon, R. F. Kefford, A. M. Menzies, G. V. Long, J. F. Thompson, J. V. Pearson, G. J. Mann, N. K. Hayward and R. A. Scolyer, *Int J Cancer*, 2019, **144**, 1049-1060.
200. X. Bonilla, L. Parmentier, B. King, F. Bezrukov, G. Kaya, V. Zoete, V. B. Seplyarskiy, H. J. Sharpe, T. McKee, A. Letourneau, P. G. Ribaux, K. Popadin, N. Basset-Seguin, R. Ben Chaabene, F. A. Santoni, M. A. Andrianova, M. Guipponi, M. Garieri, C. Verdan, K. Grosdemange, O. Sumara, M. Eilers, I. Aifantis, O. Michielin, F. J. de Sauvage, S. E. Antonarakis and S. I. Nikolaev, *Nature Genet.*, 2016, **48**, 398-+.
201. S. S. Jayaraman, D. J. Rayhan, S. Hazany and M. S. Kolodney, *J Invest Dermatol*, 2014, **134**, 213-220.
202. S. Durinck, C. Ho, N. J. Wang, W. Liao, L. R. Jakkula, E. A. Collisson, J. Pons, S. W. Chan, E. T. Lam, C. Chu, K. Park, S. W. Hong, J. S. Hur, N. Huh, I. M. Neuhaus, S. S. Yu, R. C. Grekin, T. M. Mauro, J. E. Cleaver, P. Y. Kwok, P. E. LeBoit, G. Getz, K. Cibulskis, J. C. Aster, H. Y. Huang, E. Purdom, J. Li, L. Bolund, S. T. Arron, J. W. Gray, P. T. Spellman and R. J. Cho, *Cancer Discov.*, 2011, **1**, 137-143.
203. C. L. Jones, A. Degasperi, V. Grandi, T. D. Amarante, C. Genomics England Research, T. J. Mitchell, S. Nik-Zainal and S. J. Whittaker, *Sci Rep*, 2021, **11**, 3962.
204. N. K. Hayward, J. S. Wilmott, N. Waddell, P. A. Johansson, M. A. Field, K. Nones, A. M. Patch, H. Kakavand, L. B. Alexandrov, H. Burke, V. Jakrot, S. Kazakoff, O. Holmes, C. Leonard, R. Sabarinathan, L. Mularoni, S. Wood, Q. Y. Xu, N. Waddell, V. Tembe, G. M. Pupo, R. De Paoli-Iseppi, R. E. Vilain, P. Shang, L. M. S. Lau, R. A. Dagg, S. J. Schramm, A. Pritchard, K. Dutton-Regester, F. Newell, A. Fitzgerald, C. A. Shang, S. M. Grimmond, H. A. Pickett, J. Y. Yang, J. R. Stretch, A. Behren, R. F. Kefford, P. Hersey, G. V. Long, J. Cebon, M. Shackleton, A. J. Spillane, R. P. M. Saw, N. Lopez-Bigas, J. V. Pearson, J. F. Thompson, R. A. Scolyer and G. J. Mann, *Nature*, 2017, **545**, 175-180.
205. A. H. Shain and B. C. Bastian, *Nature Rev. Cancer*, 2016, **16**, 345-358.
206. N. D. Sharma and R. J. H. Davies, *J. Photochem. Photobiol. B: Biol.*, 1989, **3**, 247-258.
207. S. Asgatay, A. Martinez, S. Coantic-Castex, D. Harakat, C. Philippe, T. Douki and P. Clivio, *J. Am. Chem. Soc.*, 2010, **132**, 10260-10261.